

Analytic Model of Capture Probability for Salvo of Two Electromagnetic Launched Anti-torpedo Torpedoes

Baoqi Wu, Xiaocun Guan* and Shaohua Guan

*National Key Laboratory of Science and Technology on Vessel Integrated Power System, Naval University of Engineering,
Wuhan - 430 033, China*

**E-mail: guanxiaocun2012@163.com*

ABSTRACT

To pre-estimate the capture probability of electromagnetic coil salvo two anti-torpedo torpedoes (ATTs), an analytic model is proposed. Based on the analysis of the influencing factors, including the target position dispersion of the incoming torpedo, the entry point's dispersion of the electromagnetic launched ATT, the underwater tracking speed and heading error of the ATT, and the differences between the salvo and single launch mode, a single integral analytic model of the capture probability is established. The course errors of the ATTs are comprehensively calculated utilizing search model, and the search boundaries of the two ATTs are calculated using the geometric method, taking the optimal searching course of the virtual single launch ATT as the desired searching course of the parallel salvo of the two ATTs. The calculation results of the proposed analytic model are consistent with the statistical results of the Monte Carlo approach through simulation comparison and analysis. The proposed analytic model's consequences for decision-making and effect assessment are discussed.

Keywords: Electromagnetic launch; Anti-torpedo torpedo; Analytic model; Salvo of two ATT

1. INTRODUCTION

An induction coil launcher is an important application of Electromagnetic Launch (EML) technology, as a kind of new launch technology¹, which can convert the electric energy, stored in the pulse power supply, into the kinetic energy of the launched projectile. A typical multi-stage coil launcher is composed of driving circuits, multi-stages coils, a launcher body, and supporting servo equipment²⁻³. Through the orderly discharge of coils at each stage, the projectile generates induced eddy in the changing magnetic field. And it is accelerated by each stage until out of the launcher muzzle. The EML technology has the characteristics of strong energy controllability, high conversion efficiency, modular structure, and cuttability, and will not leave any spray impurities on the deck during launch. The electromagnetic induction coil launcher can be used to launch the ship borne Anti-Torpedo Torpedo (ATT) to accelerate approaching the enemy, expand the defense range, and enhance the platform's defense ability against incoming torpedoes⁴.

Capture probability is an important index to evaluate ATT combat capability. Conventional capture probability calculation methods include the Monte Carlo method and the analytic model method⁵. The Monte Carlo method is a kind of calculation method based on statistics, and it is affected by the times of simulations, which requires a large amount of simulation⁶⁻⁸. By establishing an analytic model and taking the combat background, equipment performance, and battlefield

situation as input parameters, the capture probability results can be directly calculated. Different from Monte Carlo method, the analytic calculation is a kind of pre-calculation method, which applies to the prediction and decision-making of weapon combat effectiveness in wartime⁹⁻¹⁰.

Salvo refers to launching two or more homing weapons in a short time. By parallel searching the target, the effective search range is expanded to improve the capture probability¹¹. At present, salvo has become a common method used in the operation of homing weapons. In the current research on the analytic models of capture probability, the torpedoes can be divided into rocket-assisted torpedo and aerial torpedo according to the launching mode, and the torpedoes can be divided into acoustic homing torpedo and wake homing torpedo according to the homing mode. When establishing analytic models for various types of torpedoes, the focus is to establish the capture probability density function. For rocket-assisted torpedoes and aerial torpedoes, the density function is usually in the form of a double integral about the coordinates of the torpedo entry point¹².

For the rocket-assisted torpedo,¹³ has established the analytic models of the salvo capture probability under the advanced point and the current point firing modes respectively, and on this basis, an artificial dispersion salvo firing method is proposed. Because the entry point of the rocket-assisted torpedo is far from the launch platform, and the torpedo is under dynamic control in the air, the dispersion of the torpedo's entry point is usually approximated the circular dispersion when modeling. For acoustic homing and wake homing torpedoes, the probability density function is usually in the

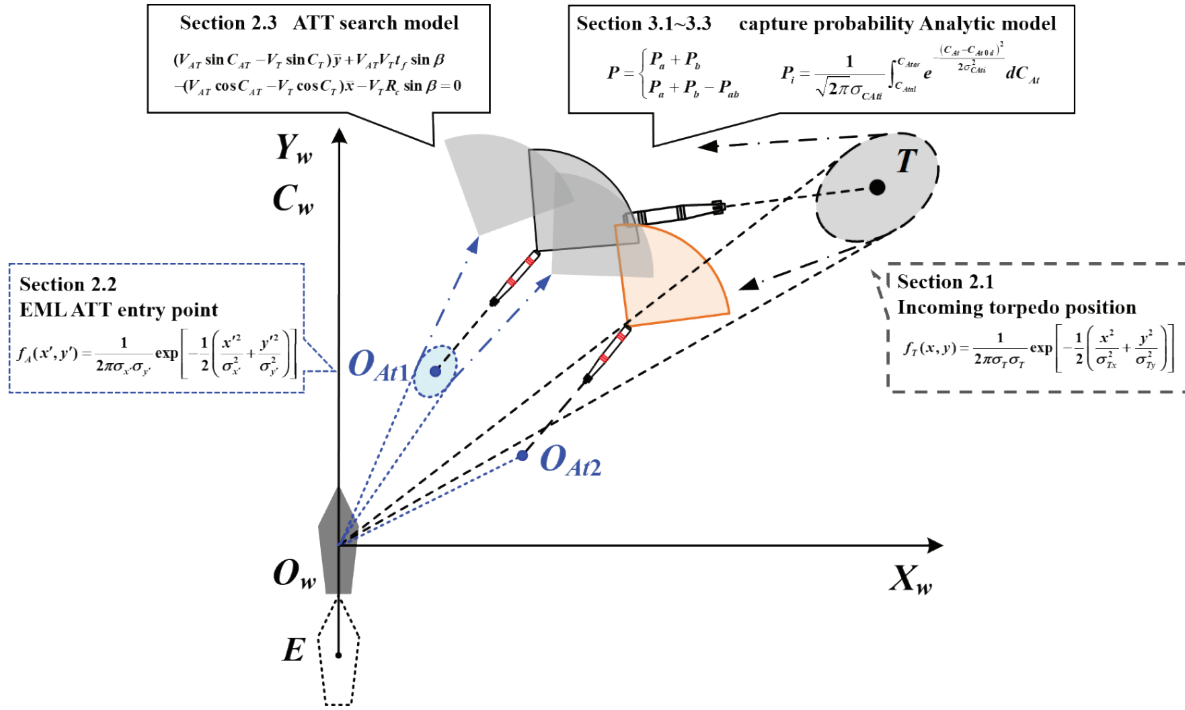


Figure 1. Schematic overview of the research.

form of an integral about the torpedo’s underwater searching course. According to the torpedo’s underwater searching process¹⁴, proposed a quadruple integral calculation model of acoustic homing torpedo’s salvo capture probability, and the feasibility of the model was verified. On this basis¹⁵⁻¹⁶, in the motion variable error and rotation angle error of the torpedo are converted to the torpedo course, and a single integral calculation model is established for the acoustic homing torpedo and the wake homing salvo torpedo respectively. However, the integral boundaries are generally approximately calculated with the bisection iteration method, as it is difficult to derive a mathematical calculation method.

The paper focuses on establishing the analytic model of the capture probability of electromagnetic salvo ATT. Based on previous research¹⁷, the main influencing factors of the capture probability of ATT salvo are analysed. According to the error of the electromagnetic launcher, the dispersion error of two ATTs’ entry points during salvo is analysed. According to the relative positions of the incoming torpedo and the ship, the underwater course of the virtual single shot ATT is calculated and taken as the desired course of the salvo ATT. The heading errors of two ATTs are calculated synthetically according to the target position dispersion error, the entry points dispersion error, and the ATT navigation error. The geometric method is adopted to calculate the searching course boundaries of the two ATTs. According to the situation of the search boundaries of the two ATTs, an analytic model of the capture probability of salvo is derived. The validity of the model is proven by comparing the results of the analytic model with the results of the Monte Carlo. The research overview is shown in Fig. 1.

2. INFLUENCING FACTORS ANALYSIS

2.1 EML Salvo ATTs and the Errors

After diving into the water, adjusting its attitude,

and turning into the direct course searching section, the electromagnetic launched ATT searches for the incoming torpedo according to the course calculated by the control equipment on the warship. In single launch mode, the ATT’s searching heading is the same as the EMLazimuth¹⁷. In salvo mode, the flight segment can be used to achieve the expansion of the two ATT, by adjusting the launching azimuth angles of the two ATTs, as shown in Fig. 2. The EML range is L_p , the expansion angle is 2δ , and the desired virtual single launched ATT’s searching course is C_{A0d}

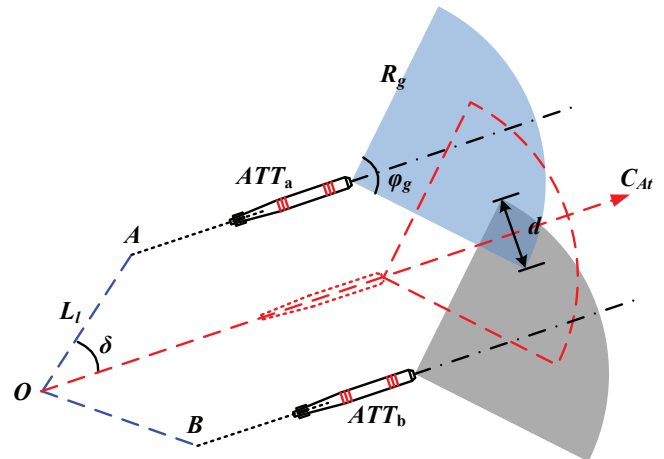


Figure 2. ATTs achieve salvo expansion by using the EML.

Therefore, the launching parameters to be calculated include the EML range, launching azimuth angles, and the straight searching course. When calculating the launching parameters of salvo, the intermediate calculation can be carried out by supposing the virtual single launched ATT, as shown in Fig. 2. The searching heading of the virtual single ATT is

regarded as the desired searching heading of the salvo. On this basis, δ is calculated, i.e., the launching azimuth angles of two ATTs are obtained. To make full use of the searching width of either ATT, a fixed spacing distance d_{in} between two ATT is usually preset. Then the angle between EML azimuth angle of either ATT and the virtual ATT is

$$\delta = \arcsin\left(\frac{d_{in}}{2L_{max}}\right) \quad (1)$$

where, d_{in} shall be determined according to ATTs' homing capability. The maximum EML range L_{max} is taken as the launching range. To prevent the target escaping from the gap between the two ATT homing sectors, certain areas between the two ATT homing sectors are usually kept overlapping. Then the launching azimuth angles of the two ATTs can be calculated as

$$\psi_{a,b} = C_{At} \pm \delta \quad (2)$$

From the induction coil launcher model, by changing the supply voltage and the launching pitch angle, the projectile's launching range can be adjusted. Under the same conditions, the relationship between the maximum EML range of the virtual injective and the salvo is

$$L'_{max} = L_{max} \cos \delta \quad (3)$$

According to the operational process of the EML salvo ATTs, the deviation is mainly influenced by the detection error, the data processing and calculation error from the control equipment of the warship, the error of launcher servo and the charging voltage, the error of ATT underwater tracking speed and heading control, etc. These errors have a comprehensive effect on ATT's capture probability of the incoming torpedo. However, the calculation error of data can be controlled within a very small range and can be ignored.

2.2 Position of the Incoming Torpedo

The target detection error is mainly determined by the sensor's performance of the platform, including the detecting range error σ_{DT} and bearing error σ_{BT} . In cartesian coordinates, the position error of the target can be derived with σ_{DT} and the σ_{BT} . It is obtained by the rotation transformation, expressed as

$$\begin{aligned} \sigma_{Tx}^2 &= \sigma_{DT}^2 \sin^2 B + \sigma_{BT}^2 D_T^2 \cos^2 B \\ \sigma_{Ty}^2 &= \sigma_{DT}^2 \cos^2 B + \sigma_{BT}^2 D_T^2 \sin^2 B \end{aligned} \quad (4)$$

where, σ_{Tx} and σ_{Ty} represent the position deviation of the incoming torpedo along the axes. D_T and B_T represent the target distance and bearing respectively.

The position error of the incoming torpedo is determined by the detection performance of the ship's underwater acoustic system, which has no relationship to the launching azimuth and EML range of ATT. Therefore, the position error expression remains unchanged in different launching modes¹⁷.

2.3 EML ATT Entry Point

The deviation of ATT's entry point includes axial and radial deviation along the launching tube, of which the radial deviation is mainly determined by the error of launching

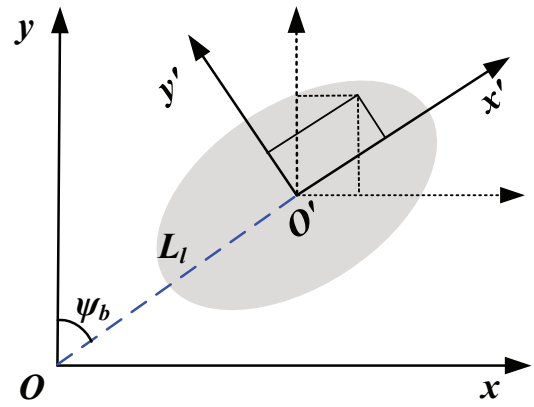


Figure 3. Transformation of entry point dispersion.

azimuth, while the axial deviation is mainly determined by the error of EML range, the deviation of launching pitch angle, and the charging voltage of pulse power supply.

$$\begin{aligned} \Delta x' &= (L_i + \Delta L) \cos(\Delta\psi) - L_i \\ &= \Delta L \cos \Delta\psi - L_i \sin^2(\Delta\psi/2) \\ \Delta y' &= (L_i + \Delta L) \sin(\Delta\psi) \\ &= L_i \sin \Delta\psi + \Delta L \sin \Delta\psi \end{aligned}$$

As shown in Fig. 3, in any launching direction ψ_b , in the reference frame $x'o'y'$, the point of entry deviation can be calculated as

ΔL represents EML range error and $\Delta\psi$ represents launch azimuth error, and the two variables are mutually independent. If the small quantity of second order is ignored, it can be obtained

$$\begin{aligned} \Delta x' &= \Delta L \cos \Delta\psi \\ \Delta y' &= L_i \sin \Delta\psi \end{aligned} \quad (5)$$

Thus the variance of the entry point deviation can be expressed as

$$\begin{aligned} \sigma_{x'}^2 &= \sigma_L^2 \\ \sigma_{y'}^2 &= L^2 \sigma_\psi^2 \end{aligned} \quad (6)$$

where, the σ_L represents the error of EML range and σ_ψ represents the error of the launching azimuth. Through coordinate transformation, the entry point deviation in frame xoy can be obtained:

$$\begin{bmatrix} \Delta x \\ \Delta y \end{bmatrix} = \begin{bmatrix} \sin \psi & -\cos \psi \\ \cos \psi & \sin \psi \end{bmatrix} \begin{bmatrix} \Delta x' \\ \Delta y' \end{bmatrix}$$

Expand the matrix, the error can be derived

$$\begin{aligned} \Delta x &= \Delta L \cos \Delta\psi \sin \psi - L_i \sin \Delta\psi \cos \psi \\ \Delta y &= \Delta L \cos \Delta\psi \cos \psi + L_i \sin \Delta\psi \sin \psi \end{aligned} \quad (7)$$

For EML salvo of two ATTs, without loss of generality, the left ATT along the search heading is defined as a#ATT, and the right is defined as b#ATT, then

$$\psi_{a,b} = \psi \mp \delta$$

The entry points are $A(x_A, y_A)$ and $B(x_B, y_B)$. And the deviation of point A is

$$\begin{bmatrix} \Delta x_A \\ \Delta y_A \end{bmatrix} = \begin{bmatrix} \sin(\psi - \delta) & -\cos(\psi - \delta) \\ \cos(\psi - \delta) & \sin(\psi - \delta) \end{bmatrix} \begin{bmatrix} \Delta x' \\ \Delta y' \end{bmatrix}$$

By expanding and substituting with Eqn.7, the deviation of point A in X-axis direction can be obtained

$$\begin{aligned} \Delta x_A &= \Delta L \cos \Delta \psi (\sin \psi \cos \delta - \cos \psi \sin \delta) \\ &\quad - L \sin \Delta \psi (\cos \psi \cos \delta + \sin \psi \sin \delta) \\ &= \cos \delta \Delta x - \sin \delta \Delta y \end{aligned}$$

The deviation of entry point A in the Y-axis direction can be obtained similarly.

$$\Delta y_A = \sin \delta \Delta x + \cos \delta \Delta y$$

In the same way, the deviation of entry point B can be obtained:

$$\begin{aligned} \Delta x_B &= \cos \delta \Delta x + \sin \delta \Delta y \\ \Delta y_B &= -\sin \delta \Delta x + \cos \delta \Delta y \end{aligned}$$

Furtherly, the variance of Δx_A is calculated by definition

$$\sigma_{x_A}^2 = E(\Delta x_A^2) - (E\Delta x_A)^2$$

where, $E\Delta x_A = 0$, and the formula above can be expanded as

$$\begin{aligned} \sigma_{x_A}^2 &= E[(\cos \delta \Delta x - \sin \delta \Delta y)^2] \\ &= E[(\cos \delta (\sin \psi \Delta x' - \cos \psi \Delta y') - \sin \delta (\cos \psi \Delta x' + \sin \psi \Delta y'))^2] \\ &= \sin^2(\psi - \delta) E(\Delta x'^2) + \cos^2(\psi - \delta) E(\Delta y'^2) \end{aligned}$$

Substituting $\sigma_{x'}^2$ and $\sigma_{y'}^2$, it can be derived

$$\sigma_{x_A}^2 = \sin^2(\psi - \delta) \sigma_L^2 + \cos^2(\psi - \delta) L^2 \sigma_\psi^2 \quad (8)$$

Similarly, the variance of Δy_A can be calculated as

$$\sigma_{y_A}^2 = \cos^2(\psi - \delta) \sigma_L^2 + \sin^2(\psi - \delta) L^2 \sigma_\psi^2 \quad (9)$$

In the same way, the variance of the deviation of point B is

$$\begin{aligned} \sigma_{x_B}^2 &= \sin^2(\psi + \delta) \sigma_L^2 + \cos^2(\psi + \delta) L^2 \sigma_\psi^2 \\ \sigma_{y_B}^2 &= \cos^2(\psi + \delta) \sigma_L^2 + \sin^2(\psi + \delta) L^2 \sigma_\psi^2 \end{aligned} \quad (10)$$

2.4 ATT Search Model

The position of the incoming torpedo can be expressed as

$$\begin{aligned} x_T &= x_{T0} + V_T t \sin C_T \\ y_T &= y_{T0} + V_T t \cos C_T \end{aligned} \quad (11)$$

The (x_T, y_T) represents the position of the incoming torpedo; V_T represents the speed of the incoming torpedo. Define the moment the warship launches the ATTs as initial, then $t = t_f + t_s$, where t_f is the flying time of ATT in the air, and t_s is the ATT's tracking time of straight searching underwater.

For virtual single launched ATT, the reference capture point of its homing sector after entering water can be expressed as:

$$\begin{aligned} x_g &= x_{O'} + (V_{At} t_s + \lambda R_g) \sin C_{At} \\ y_g &= y_{O'} + (V_{At} t_s + \lambda R_g) \cos C_{At} \end{aligned} \quad (12)$$

$(x_{O'}, y_{O'})$ represents the coordinates of the entry point; V_{At} is ATT speed; R_g refers to the ATT homing distance; λR_g refers

to the distance from the reference capture point to the ATT head, C_{At} is the searching course of ATT.

When the reference capture point of the ATT homing sector coincides with the position of the incoming torpedo, it is considered that ATT has captured the target

$$\begin{aligned} x_T &= x_g \\ y_T &= y_g \end{aligned} \quad (13)$$

Combine Eqn. 12 and Eqn. 13, ATT's search model can be obtained when eliminating t_s .

$$\begin{aligned} (V_{At} \cos C_{At} - V_T \cos C_T)(x_{T0} - x_{O'}) - \\ (V_{At} \sin C_{At} - V_T \sin C_T)(y_{T0} - y_{O'}) \\ + (\lambda R_g - V_{At} t_f) V_T \sin(C_{At} - C_T) = 0 \end{aligned} \quad (14)$$

The theoretical searching heading C_{At0d} can be calculated according to , and defined as the desired searching heading for either ATT. The required variables include V_{At} , V_T , C_T , x_{T0} , y_{T0} , $x_{A'}$, $y_{A'}$. V_{At} is determined by ATT performance. V_T , C_T and $x_{O'}$, $y_{O'}$ can be detected and calculated, and x_{T0} , y_{T0} can be detected by the sensor, t_f depends on the exterior ballistics of the projectile.

3. ANALYTIC MODEL

3.1 Search Course Variance

When establishing the analytic model of capture probability for a#ATT, the influencing factors are considered comprehensively. Let the left part of the searching model be

$$\begin{aligned} f &= (V_{At} \cos C_{Ata} - V_T \cos C_T) \bar{x} - (V_{At} \sin C_{Ata} - V_T \sin C_T) \bar{y} \\ &\quad + (\lambda R_g - V_{At} t_f) V_T \sin \beta \end{aligned} \quad (15)$$

where, $\bar{x} = x_{T0} - x_{A'}$, $\bar{y} = y_{T0} - y_{A'}$, $\beta = C_{Ata} - C_T$. Using the implicit function differentiation, $\sigma_{C_{Ata}}$ can be calculated as:

$$\begin{aligned} \sigma_{C_{Ata}}^2 &= \left(\frac{\partial f / \partial t_f}{\partial f / \partial C_{Ata}} \right)^2 \sigma_{t_f}^2 + \left(\frac{\partial f / \partial x_{T0}}{\partial f / \partial C_{Ata}} \right)^2 \sigma_{x_{T0}}^2 + \left(\frac{\partial f / \partial y_{T0}}{\partial f / \partial C_{Ata}} \right)^2 \sigma_{y_{T0}}^2 + \left(\frac{\partial f / \partial x_{A'}}{\partial f / \partial C_{Ata}} \right)^2 \sigma_{x_{A'}}^2 \\ &\quad + \left(\frac{\partial f / \partial y_{A'}}{\partial f / \partial C_{Ata}} \right)^2 \sigma_{y_{A'}}^2 + \left(\frac{\partial f / \partial V_{At}}{\partial f / \partial C_{Ata}} \right)^2 \sigma_{V_{At}}^2 + \left(\frac{\partial f / \partial V_T}{\partial f / \partial C_{Ata}} \right)^2 \sigma_{V_T}^2 + \left(\frac{\partial f / \partial C_T}{\partial f / \partial C_{Ata}} \right)^2 \sigma_{C_T}^2 \end{aligned} \quad (16)$$

and the partial derivatives are expressed as:

$$\begin{aligned} \partial f / \partial t_f &= -V_{At} V_T \sin \beta \\ \partial f / \partial x_{T0} &= V_{At} \cos C_{Ata} - V_T \cos C_T \\ \partial f / \partial y_{T0} &= -(V_{At} \sin C_{Ata} - V_T \sin C_T) \\ \partial f / \partial x_{A'} &= -(V_{At} \cos C_{Ata} - V_T \cos C_T) \\ \partial f / \partial y_{A'} &= V_{At} \sin C_{Ata} - V_T \sin C_T \\ \partial f / \partial V_{At} &= \cos C_T \bar{x} - \sin C_T \bar{y} - V_T t_f \sin \beta \\ \partial f / \partial V_T &= -\cos C_T \bar{x} + \sin C_T \bar{y} - V_{At} t_f \sin \beta + \lambda R_g \sin \beta \\ \partial f / \partial C_T &= V_T \sin C_T \bar{x} + V_T \cos C_T \bar{y} + (V_{At} V_T t_f - \lambda R_g V_T) \cos \beta \\ \partial f / \partial C_{At} &= -V_{At} \sin C_{Ata} \bar{x} - V_{At} \cos C_{Ata} \bar{y} - (V_{At} V_T t_f - \lambda R_g V_T) \cos \beta \end{aligned}$$

$\sigma_{C_{Atb}}$ can be computed similarly.

3.2 Integral Boundary

The integral boundaries calculation was carried out by using the geometric method¹⁷. As shown in Fig. 4, taking the entry point A as the center, ATT rated speed $|V_{At}|$ as the radius,

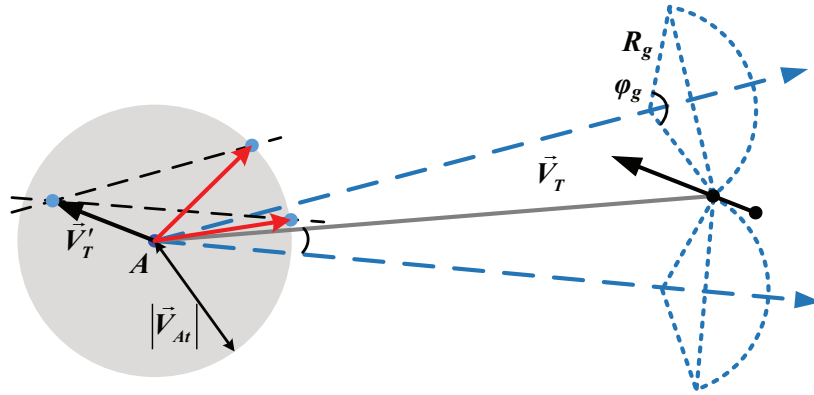


Figure. 4 Searching heading boundaries of ATT rated speed.

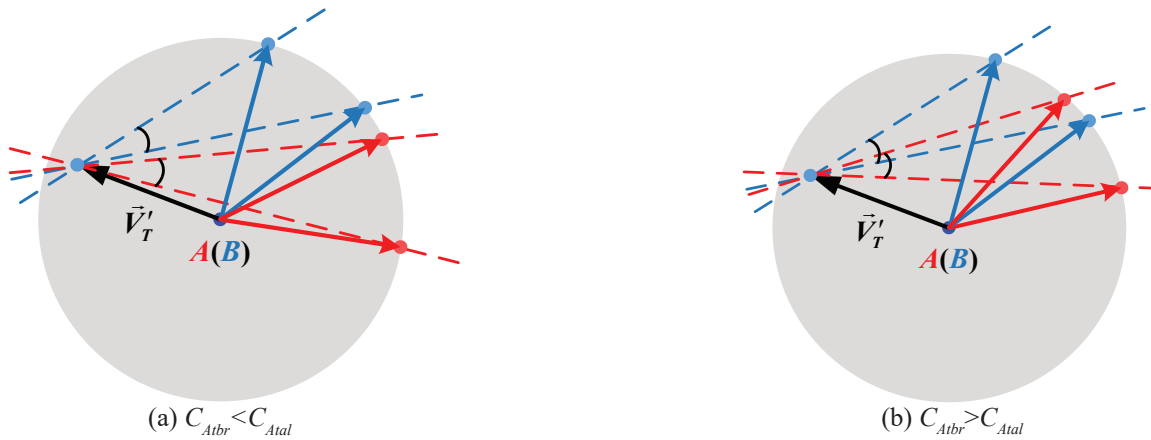


Figure 5. Searching boundaries of the two ATTs.

and the navigation circle $\odot A$ is defined. According to the position and relative motion of ATT and the incoming torpedo, the limiting searching headings C'_{Atl} and C'_{Atr} of ATT relative to the incoming torpedo are obtained; Translating the origin of the incoming torpedo's velocity vector to Point A, a vector V'_T is obtained; Through the terminal points of V'_T , draw two straight lines l_{al} and l_{ar} parallel to C'_{Atl} and C'_{Atr} , respectively, intersecting $\odot A$ at point P_{al} and P_{ar} . The direction angle of vector AP_{al} and AP_{ar} are the left searching heading boundary C_{Atal} and right boundary C_{Atrar} of a#ATT respectively. The heading boundaries C_{Atbl} and C_{Atrb} of b# ATT can be obtained with the same approach.

The desired searching heading of ATT to the target is determined by the positions of the ATT and the incoming torpedo. The included angle between the relative searching heading boundary and the relative desired searching heading can be calculated as:

$$\delta_b = \arcsin\left(\frac{R_g \sin(\varphi_g/2)}{D_{AT}}\right)$$

where, D_{AT} represents the distance between the entry point and the incoming torpedo. Move $\odot A$ and $\odot B$ to coincide. l_{bl} and l_{br} are corresponding to the left and right relative searching heading boundaries of b#ATT, and the intersection points with the $\odot B$ are P_{bl} and P_{br} respectively. There are two scenarios, as shown in Fig. 5.

3.3 Analytic Model

For the EML salvo ATTs, the anti-torpedo combat is considered successful if either ATT captures the incoming torpedo. Thus, the analytic model of capture probability of EML salvo ATTs can be given:

$$P = \begin{cases} P_a + P_b & C_{Atbl} < C_{Atrb} \leq C_{Atal} < C_{Atrar} \\ P_a + P_b - P_{ab} & C_{Atbl} < C_{Atal} < C_{Atrb} < C_{Atrar} \end{cases}$$

$$P_a = \frac{1}{\sqrt{2\pi}\sigma_{C_{Ata}}} \int_{C_{Atal}}^{C_{Atrar}} e^{-\frac{(C_{Ata}-C_{At0d})^2}{2\sigma_{C_{Ata}}^2}} dC_{Ata}$$

$$P_b = \frac{1}{\sqrt{2\pi}\sigma_{C_{Atb}}} \int_{C_{Atbl}}^{C_{Atrb}} e^{-\frac{(C_{Atb}-C_{At0d})^2}{2\sigma_{C_{Atb}}^2}} dC_{Atb} \quad (17)$$

where, P_a and P_b refer to the capture probability of a# and b#ATT respectively. P_{ab} refers to the capture probability of a# and b# ATT simultaneously. P is the capture probability of EML salvo ATTs.

It is obvious that, when C_{At0d} , $\sigma_{C_{Ata}}$ and $\sigma_{C_{Atb}}$ are calculated, P_a , P_b can be directly calculated by the normal distribution probability function. When $C_{Atrb} > C_{Atal}$, the two ATTs will capture the incoming torpedo at the same time. Since the searching heading variances of the two ATTs are different, the capture probability density functions are different in shape, thus P_{ab} needs to be calculated in different cases.

For the two cases shown in Fig. 6, the shaded area represents the probability that both ATTs can capture the incoming torpedo, which can be calculated as:

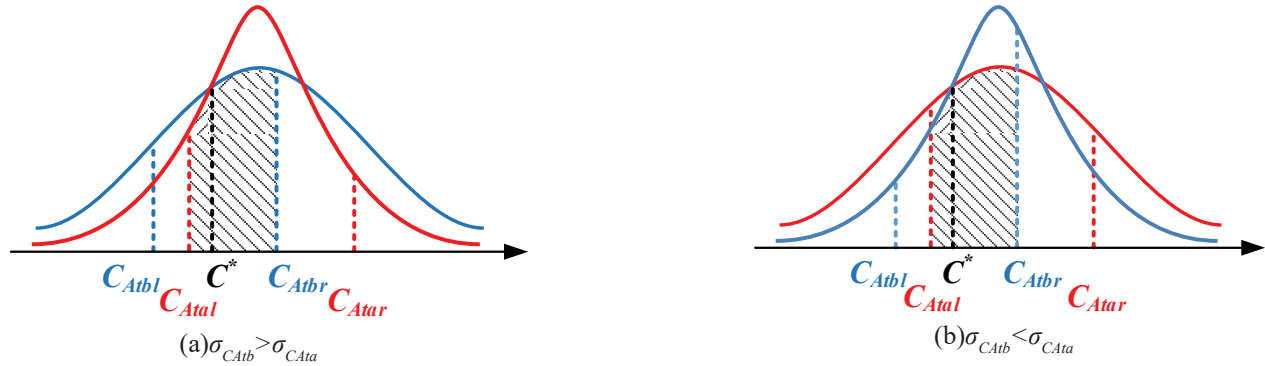

 Figure 6. Two calculation cases of P_{ab} .

Table 1. Simulation parameter settings

The warship			Anti-torpedo torpedo			Incoming torpedo		
heading	C_w	0°	speed	V_{At}	50 kn	alarming distance	D_T	3 km~8 km
speed	V_w	20 kn	reaction time	t_r	30 s	target bearing	B_T	$30^\circ \sim 150^\circ$
distance error	σ_D	5 %	maximum EML range	L_{lmax}	1200 m	rated speed	V_T	45 kn
bearing error	σ_Q	3°	velocity error	σ_{VAT}	0.5 kn	heading error	σ_{CT}	2°
launch range error	σ_L	3 %	homing distance	R_g	600 m	speed error	σ_{VT}	2 kn
launch azimuth error	σ_ψ	1°	homing opening angle	ϕ_g	60°			

$$P_{ab} = \begin{cases} \frac{1}{\sqrt{2\pi}\sigma_{CAta}} \int_{C_{Atal}}^{C^*} e^{-\frac{(C_{Ata}-C_{At0d})^2}{2\sigma_{CAta}^2}} dC_{Ata} + \\ \frac{1}{\sqrt{2\pi}\sigma_{CAtb}} \int_{C_{Atal}}^{C^*} e^{-\frac{(C_{Atb}-C_{At0d})^2}{2\sigma_{CAtb}^2}} dC_{Atb} + \\ \frac{1}{\sqrt{2\pi}\sigma_{CAtb}} \int_{C^*}^{C_{Atr}} e^{-\frac{(C_{Atb}-C_{At0d})^2}{2\sigma_{CAtb}^2}} dC_{Atb} & \sigma_{CAtb} > \sigma_{CAta} \\ \frac{1}{\sqrt{2\pi}\sigma_{CAta}} \int_{C^*}^{C_{Atr}} e^{-\frac{(C_{Ata}-C_{At0d})^2}{2\sigma_{CAta}^2}} dC_{Ata} & \sigma_{CAtb} < \sigma_{CAta} \end{cases}$$

where, C^* is the abscissa of the intersection point of the two probability density functions, which can be obtained

$$C^* = C_{At0d} - \frac{2\sigma_{CAta}^2\sigma_{CAtb}^2(\ln\sigma_{CAta} - \ln\sigma_{CAtb})}{(\sigma_{CAta}^2 - \sigma_{CAtb}^2)} \quad (18)$$

According to the value of σ_{CAta} , σ_{CAtb} , C_{Atr} , C_{Atal} , and C^* , there are several calculation cases of P_{ab} , which will not be described perpetually here.

4. SIMULATION AND ANALYSIS

4.1 Analytic Model and Results Analysis

To verify the effectiveness of the proposed salvo analytic model, under the typical anti-torpedo combat situation, the capture probability results calculated by the analytic model are investigated. The trend and influencing factors of the capture probability are analyzed and compared with the statistical results of Monte Carlo method.

The parameter settings include the warship, ATT and incoming torpedo part. The specific parameters are shown in Table 1.

The capture probability result calculated by the analytic model is shown in Figure 7, and each result curve changes

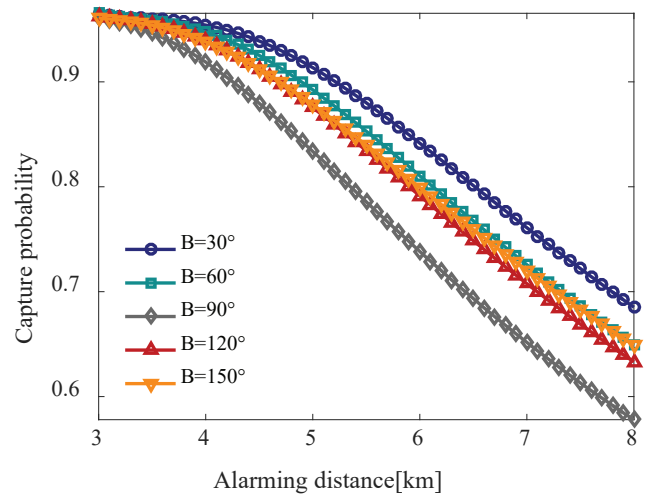


Figure 7. Analytic model results with different alarming distances and bearings.

regularly with the target distance and bearing. The capture probability varies from 0.57 to more than 0.95 overall.

The results reveal that the capture probability decreases with the increasing alarming distance of the target. Specifically, when the initial distance of the target is 3km, the capture probability can reach more than 0.96 for incoming targets at different bearings; When the initial target distance increases to 8 km, the capture probability decreases to 0.57~0.69; The capture probability varies with the bearing of the target, and the capture probability of the forward and stern incoming targets is higher than that from the side. Specifically, when the target's alarming distance stays unchanged, the capture probability of ATT with bearing at 30° is the largest, followed by 60° and 150° , and the smallest when the incoming bearing is 90° . With the same distance, the maximum difference between the capture probability of 30° and 90° bearing is about 0.11.

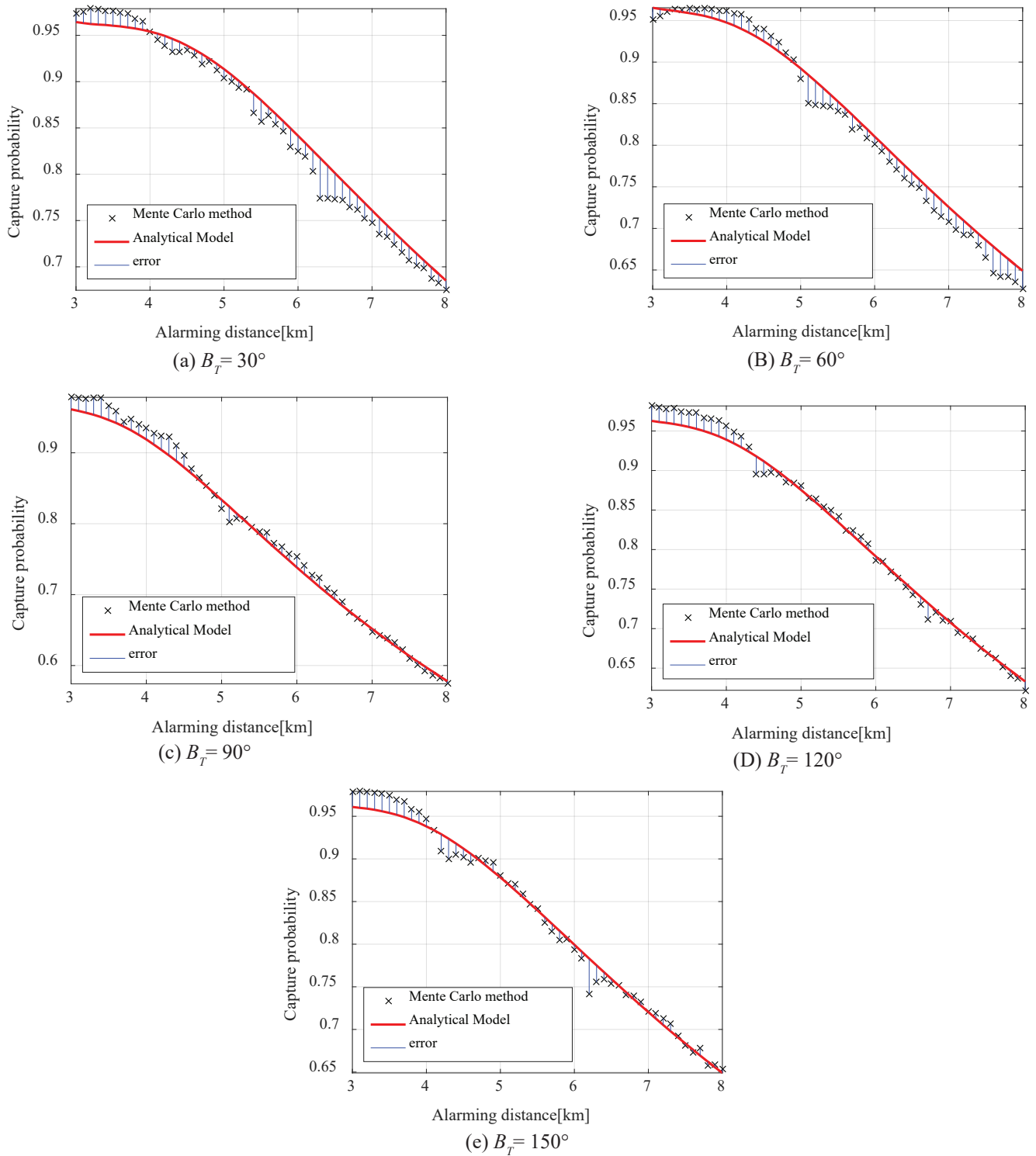


Figure 8. Results comparison between analytic model and Monte Carlo.

The calculation results indicate that the capture probability decreases with the increasing alarming distance of the incoming torpedo, which are in agreement with the existing research conclusion¹⁸. The mathematic explanation is that σ_{Tx} and σ_{Ty} are large when the alarming distance of an incoming torpedo is far according to Eqn, as a result, σ_{CAta} and σ_{CAtb} increase respectively, thus the capture probability decreases based on the capture probability density function. The capture probability varies with the changing bearing of the incoming

torpedo. The capture probability at the bow and stern of the ship is higher than that from the sideboard. This is because when the incoming torpedo attacks from the warship's sideboard, its ballistic dispersion is larger¹⁹, and the capture probability becomes smaller with an unchanged searching sector of ATT.

4.2 Comparison with Monte Carlo Results

The Monte Carlo method is used to simulate and calculate the capture probability of EML salvo ATTs. Under each

situation, the simulation is repeated 2000 times, the capture probability is compared with the calculation results of the analytic model. The comparison results are shown in Fig. 8.

It can be seen from the comparison of the results that under different incoming bearings, the capture probability trend of the analytic model corresponds to the results obtained by Monte Carlo. The results show that the difference of the values with different methods is small; however, the calculation result curve of the analytic model is more continuous and smooth. When $3\text{ km} < D_T < 4\text{ km}$, the result of the Monte Carlo method is greater than that of the analytic model. When $4\text{ km} < D_T < 8\text{ km}$, the results of the two methods have no obvious regularity. For targets in all directions, the curves of analytic model calculation results are continuous and derivable, while the Monte Carlo simulation results are discrete. There exist mutations in a small range, such as (6.3 km, 30°), (5.1 km, 60°), (4.4 km, 120°), (6.2 km, 150°). The statistical errors of capture probability obtained by the two methods are shown in Table 2. The maximum deviation of results under all situations is 5.59 %, which occurs under the situation of (6.3 km, 30°); The situation with a deviation of less than 3 % accounted for about 95.29 %; The situation with a deviation of $3\% < \Delta P \leq 5\%$ accounts for about 3.92 % (mainly occurs in 7.5 km to 8.0 km, $B_T = 60^\circ$).

The comparison results of the two methods show that the calculated results of the analytic model are close to the Monte Carlo statistical results, which implies that the analytic model is effective and applicable. Nevertheless, there is a certain deviation between the different methods. On the one hand, the influence of high-order small quantity when analyzing the

position dispersion error of incoming torpedo and the error of ATT entry point is ignored. On the other hand, the statistical results of Monte Carlo method are also affected by the times of repeated simulation. The numerical results have certain randomness and cannot be considered as an absolute standard for judgment.

In addition, in the process of calculating the probability density function of the two ATTs, it is found that σ_{Tx} and σ_{Ty} account for a large proportion of the heading variance of each ATT σ_{CAr} . The two items are mainly determined by the detection accuracy of the warship. Therefore, for each ATT, the value of the two items is equal, and then the heading variance of the two ATTs σ_{CAta} and σ_{CAtb} is within a small range, especially for the long-range incoming target. And σ_{CAta} and σ_{CAtb} can be approximately equal, the classification of P_{AB} calculation can be further simplified simultaneously. On this basis, the analytic model of capture probability of multiple ATT salvo can be studied, but the further quantitative analysis is required.

5. CONCLUSIONS

In this research, the target position dispersion and ATT entry point dispersion are analyzed, and the mathematical descriptions of the two dispersion errors are given respectively. The heading variance is calculated comprehensively according to the derivation of implicit function, and the desired searching heading is calculated with the virtual single launching ATT. A geometric method based on the ATT rated speed is adopted to calculate the two ATTs' searching boundaries respectively. According to the relationship between the two ATTs' search boundaries, an analytic model of capture probability of EML

Table 2. Error statistics between analytic model and Monte Carlo

Target distance	Error $ p_A - p_M /p_M \times 100\%$	Sample statistics					Sum N	Proportion %
		30°	60°	90°	120°	150°		
[3 km, 4 km)	$\Delta p \leq 3\%$	10	10	10	10	10	50	
	$3\% < \Delta p \leq 5\%$	0	0	0	0	0	0	
	$5\% < \Delta p < 6\%$	0	0	0	0	0	0	
[4 km, 5 km)	$\Delta p \leq 3\%$	10	10	10	10	10	50	
	$3\% < \Delta p \leq 5\%$	0	0	0	0	0	0	
	$5\% < \Delta p < 6\%$	0	0	0	0	0	0	
[5 km, 6 km)	$\Delta p \leq 3\%$	10	10	10	10	10	50	
	$3\% < \Delta p \leq 5\%$	0	0	0	0	0	0	
	$5\% < \Delta p < 6\%$	0	0	0	0	0	0	
[6 km, 7 km)	$\Delta p \leq 3\%$	9	10	10	10	9	48	
	$3\% < \Delta p \leq 5\%$	0	0	0	0	0	0	
	$5\% < \Delta p < 6\%$	1	0	0	0	1	2	
[7 km, 8 km]	$\Delta p \leq 3\%$	11	5	11	11	11	49	
	$3\% < \Delta p \leq 5\%$	0	6	0	0	0	6	
	$5\% < \Delta p < 6\%$	0	0	0	0	0	0	
[3 km, 8 km]	$\Delta p \leq 3\%$	48	43	51	51	50	243	95.29 %
	$3\% < \Delta p \leq 5\%$	2	8	0	0	0	10	3.92 %
	$5\% < \Delta p < 6\%$	1	0	0	0	1	2	0.78 %

salvo ATTs is given. Comparing the capture probability of the analytic model with the Monte Carlo method, the main findings are as follows:

- The capture probability results calculated by the analytic model change with the distance and bearing of the incoming torpedo, of which the trend is consistent with the statistical results of the Monte Carlo method. Both of them decrease with the increasing alarming distance of the incoming torpedo, and the capture probability of the incoming torpedo at the bow and stern of the warship is higher than that of the sideboard;
- The difference between the calculated value of the analytic model and the statistical result of the Monte Carlo method is small, and the samples with a deviation less than 3% account for about 95.3 %;
- The calculation result curve of the analytic model is continuous and smooth. On this basis, the analytic model is an effective method for predicting and evaluating the capture probability in real-time under the variable combat situation and providing theoretical support for operational decision-making and weapon parameters optimization.

REFERENCES

1. Ma, W. & Lu, J. Thinking and study of electromagnetic launch technology. *IEEE Trans. Plasma Sci.*, 2017, **99**, 1-7.
doi:10.1109/TPS.2017.2705979.
2. Guan, X.; Wang, S.; Guan, S.; Guo, D. & Liu, B. Study on the best trigger position of multistage induction coil launcher. *IEEE Trans. Plasma Sci.*, 2019, **47**(5), 2419-2423.
doi:10.1109/tps.2018.2886218.
3. Yang, D.; Liu, Z.; Shu, T.; Yang, L.; Ouyang, J. & Shen, Z. An improved genetic algorithm for multi objective optimization of helical coil electromagnetic launchers. *IEEE Trans. Plasma Sci.*, 2018, **46**(1), 127-133.
doi: 10.1109/tps.2017.2773639.
4. Alvarez. Redesigning the SLOCUM glider for torpedo tube launching. *IEEE J. of Oceanic Eng.*, 2010, **35**(4), 984-991. doi: 10.1109/joe.2010.2057170.
5. Ajith Kumar, K.; Saravanakumar, M. & Joseph, J. Generative model for conceptual design of defence equipment. *Def. Sci. J.*, 2016, **66**(1), 81-87.
doi: 10.14429/dsj.66.9105.
6. Jomon, G.; Sinchu, P.; Ajith Kumar, K. & Santhanakrishnan, T. Towed acoustic countermeasures for defending acoustic homing torpedoes. *Def. Sci. J.*, 2019 **69**(6), 607-612. doi: 10.14429/dsj.69.13337
7. Kyung-Min, S.; Song, H.S.; Kwon, S.J. & Kim, T.G. Measurement of effectiveness for an anti-torpedo combat system using a discrete event systems specification-based underwater warfare simulator. *J. Def. Model. Simulation: Appl., Methodol., Technol.*, 2010, **8**(3), 157-171.
doi: 10.1177/1548512910390245.
8. Cao, M.; Zhao, Q. & Jiang, J. Operational effectiveness evaluation of anti-torpedo torpedo weapon system based on simulation. *J. Unm. Un. Syst.*, 2020, **28**(5), 563-570.
9. Zhu, Z.; Lei, Y. & Sarjoughian, H. UML-based combat effectiveness simulation system modeling within MDE[J]. *J. Syst. Eng. Electron.*, 2018, **29**(6), 1180-1196.
doi: 10.21629/jsee.2018.06.07.
10. Tian, H.; Cao, Q. & Hou, D. Analytical model of rocket-assisted torpedo's acquisition probability. *Acta Armamentarii*. 2013, **34**(7), 916-921.
11. Liu, S.; Wang, H. & Lu, F. Research on acquiring probability of multiple missiles by area covering parallel search. *Syst. Eng. Electron.*, 2015, **37**(10), 2286-2291.
12. Zheng, Q.; Yang, R. & Chen, J. On analytical model of airdrop torpedo's detection probability. *Electron. Opt. & Cont.* 2017, **24**(3), 16-19.
13. Tian, D.; Hou, D. & Fang, Y. Analysis of acquisition probability of rocket-assisted torpedo in different salvo modes. *Acta Armamentarii*. 2015, **36**(7), 1370-1376.
14. Lei, Z. & Yuan, F. Analytic method for computing finding probability of salvo of two acoustic homing torpedoes. *Com. Cont. & Simul.*, 2014, **36**(3), 56-60.
15. Yuan, F.; Dai, Z. & Xiao, B. An analytical calculation method of the hitting/finding probability of torpedo one-time turning-angle shooting based on error conversion. *J. Unm. Un. Syst.*, 2020, **28**(3), 303-308.
16. Yang, G. & Zhang, X. Analytic method for computing finding probability of salvo of two wake homing torpedoes. *J. Ord. Equip. Eng.*, 2016, **37**(8), 33-37.
17. Wu, B.; Guan, X.; Guan, S. & Shi, J. A capture probability analytic model for the electromagnetic launched anti-torpedo torpedo. *Def. Tech.*, 2022, **18**(2), 261-270.
doi.org/10.1016/j.dt.2020.12.006.
18. Yang, X. & Yin, W. Simulation on detection probability of submarine-launched homing torpedo based on the optimized firing model. *J. Unm. Un. Syst.*, 2018, **26**(6), 568-574.
19. Chen, Y. & Qiang, C. Solution principle and simulation analysis on trajectory dispersion of incoming torpedo. *J. Ballist.*, 2018, **30**(2), 81-85.

CONTRIBUTIONS

Dr Wu Baoqi obtained his PhD at the National Key Laboratory of Science and Technology on Vessel Integrated Power System. His research interests include: Electromagnetic launch technology, system modeling, and simulation of coil gun.

In the current study, he was involved in the search model, establishing the analytic model, carrying out the simulation, data analysis, and writing the original manuscript.

Dr Guan Xiaocun obtained his PhD and currently working with the National Key Laboratory of Science and Technology on Vessel Integrated Power System. His current research interests include: Research of coil gun, analysis of electromagnetic field, temperature field, stress field, and the design of prototypes. In the current study, he helped in the overview of the manuscript, the study objectives, and the review of the manuscript.

Dr Guan Shaohua obtained his PhD in 2021. His current research interests include: Multi-physics numerical calculation of electrical devices.

In the current study, he was involved in the analysis of the dispersion of the entry position, and the introduction concept.